Available online at www.sciencedirect.com
SCIENCE DIRECT®

Journal of the European Ceramic Society 23 (2003) 1409–1415

www.elsevier.com/locate/jeurceramsoc

Unipolar fatigue of ferroelectric lead–zirconate–titanate

C. Verdier, D.C. Lupascu*, J. Rödel

Institute of Materials Science, Darmstadt University of Technology, Petersenstr. 23, 64287 Darmstadt, Germany

Received 7 June 2002; received in revised form 5 September 2002; accepted 16 September 2002

Abstract

In multilayer actuators the ferroelectric material is known to degrade under bipolar and to some degree under unipolar electric loading. Fatigue effects due to unipolar cycling of a commercial bulk lead–zirconate–titanate up to $4{\cdot}10^8$ cycles at 2 E_c are demonstrated. Unipolar as well as bipolar polarisation and strain hysteresis loops are measured after fatigue. Bipolar measurements after cycling show a small decrease of the remnant polarisation and an increasing asymmetry of the strain hysteresis with cycle number, which is explained by an offset polarisation. This offset polarisation is reduced under application of bipolar fields. A small offset-field is also observed. Etch grooves known to occur after bipolar fatigue are not found after unipolar fatigue. The results reveal that different mechanisms are responsible for bipolar and unipolar fatigue.

Keywords: Actuators; Fatigue; Ferroelectric properties; PZT

1. Introduction

The fatigue phenomenon in ferroelectric ceramics has stimulated scientific discussions for more than a decade. Large market shares are engaged with the development of non-fatiguing multilayer actuator components and ferroelectric memories.[1,2] While bipolar fatigue is mostly encountered in ferroelectric memory devices unipolar ac loading is the predominant loading regime in multilayer actuators.

The fatigue effect under bipolar loading has been phenomenologically described by many authors (Refs. 1, 3 and 4). There is general agreement that the locally switchable polarisation is reduced and accounts for the loss of macroscopic polarisation. Two types of charge configurations may constitute obstacles to domain wall motion, isolated charged defects or defect dipoles. Both types may agglomerate. Robels and Arlt explained the pinning of domain walls by the local interaction of bulk domains with charged point defect dipoles distributed within the interior of each domain.[5,6] All other models have considered the interaction of isolated or agglomerated point charges located at some perimeter of a domain. Brennan proposed the domain walls within each grain to be the location of these charges.[7] He considered the oxygen vacancy to be the dominant charge carrier. Other authors demonstrated the additional effect of electronic charge carriers either injected from the electrodes or generated from the ionization of dopants and oxygen vacancies by different processes like UV illumination.[8,9] At the present stage, this discussion has not been fully settled. The agglomeration of point defects is considered additionally necessary to fully clamp domains in bulk material an effect derived by us from etch grooves identified in bipolar fatigued samples.[3] Such a fatigue mechanism was independently predicted by Scott and Dawber as a major fatigue mechanism in the bulk of thin film ferroelectrics[10] as well as underneath the external electrodes[11] and indirectly already implied in the original model assumptions by Brennan.[7] Defects can also be seen as the source of new domain walls, if switching is assumed to be determined by domain wall generation.[12] Due to fatigue the generation process of new domain wall surface may be hindered, because the number of such domain wall sources may be reduced.[4] This may equally be the case for domain walls generated at external electrodes[13] as well as internal boundaries like e.g. 90° domain walls or grain boundaries.[14]

* Corresponding author. Tel.: +49-6151-166316; fax: +49-6151-166314.
E-mail address: lupascu@ceramics.tu-darmstadt.de (D.C. Lupascu).

0955-2219/02/$ - see front matter © 2002 Elsevier Science Ltd. All rights reserved.
PII: S0955-2219(02)00351-5

In addition to the well described mechanical failure mechanisms due to cracking,[2,15,16] the changes in material properties due to unipolar electric loading have not been addressed. This may be surprising, because the poling of a ceramic material is not complete during a single poling cycle. A subsequent increase of the polarisation state[17] entailing an increased piezoelectric coefficient during use[18] is not desired in actual electrical control circuitry.[2] Other materials exhibit the reverse effect and lose some of their switchable polarization[19] entailing a reduced piezoelectric actuation amplitude. In different fatigue studies the effect of unipolar cyclic loading on switchable polarisation has been shown to be much less pronounced than for bipolar fatigue.[20–22] No strain measurements in ceramics have been reported.

The aim of this study is to investigate the effects induced by a unipolar cyclic loading on the polarisation and strain properties of a commercial bulk PZT. In particular subsequent bipolar loading is applied to highlight the changes in switching properties caused by unipolar fatigue.

2. Experimental

2.1. Material

All measurements were performed on a commercial material (PIC 151, PI Ceramic Lederhose, Germany). The samples are disc shaped with 10 mm in diameter and 1 mm thickness. They consist of material of the ternary phase system $Pb(Ni_{1/3}Sb_{2/3})O_3$–$PbTiO_3$–$PbZrO_3$ including about 2–3% of the $Pb(Ni_{1/3}Sb_{2/3})O_3$ composition in the vicinity of the morphotropic phase boundary of PZT in the tetragonal range. The average grain size is about 6 μm.[3] All samples are electroded with silver fired into the surface at 850 °C leaving a rim of 250 μm uncovered. The Curie point is $T_c = 250$ °C. All samples were initially unpoled.

2.2. Cycling

The cycling field was 2 kV/mm (peak value). Since E_c of the uncycled material is about 1 kV/mm, this field represents approx. 2 E_c. The unipolar cyclic voltage was generated by transforming the line voltage (50 Hz, 230 V) to the desired maximum value. It was then rectified by a diode bridge rectifier in order to obtain a unipolar signal of 100 Hz. The time constant of the sample circuit was chosen such that the applied voltage reaches 0 V at the end of each waveform cycle by connecting an additional resistance in parallel to the samples. Each sample was placed between two metal clamps electrically connected to the power supply and immersed in a bath of silicon oil (Wacker-Chemie GmbH, München, Germany) in order to avoid arcing. The cycling field was steadily increased from zero to the maximum field value within 5 s. Then the peak value was held constant for a number of cycles, whereafter the field was reduced to zero again within 5 s. The samples were removed from the cycling set-up for measurement. The measurements were performed 1 h after the end of cycling in order to avoid possible differences in ageing between each sample set. Five samples were measured for each of the cycling steps (0, $2{\cdot}10^5$, 10^6, $8{\cdot}10^6$, $3.2{\cdot}10^7$, $3.2{\cdot}10^8$, $4.2{\cdot}10^8$ cycles).

2.3. Measurement

All data (polarisation, field, strain) were simultaneously recorded by the measuring set-up (AMS3, Vallen Systeme, Icking, Germany). The high voltage is delivered by a bipolar high voltage power supply (F.u.G. Elektronik GmbH, Rosenheim, Germany) driven by a frequency generator (Hewlett Packard, Santa Clara, CA, USA). The samples are placed in a silicone oil bath in order to avoid arcing. The dielectric hysteresis loops were determined by a linear capacitor ($C = 6.62\ \mu F >> C_{sample}$) placed between the sample and ground. The voltage on this capacitor was measured by an electrometer (Keithley Instruments, Cleveland, OH, USA, input resistance $10^{14}\ \Omega$) and converted to polarisation. For the strain hysteresis loops, a linear variable displacement transducer (LVDT, resolution 20 nm) connected to an ac measuring bridge (Hottinger Baldwin Meßtechnik, Darmstadt, Germany) was used. The tip of the transducer was placed onto the upper face of the sample.

In each set of five samples, bipolar measurements of the polarisation and strain hysteresis were conducted for three of them and unipolar measurements for two of them. Triangular fields of 40 mHz were used in both cases and driven to maximal values of ±2 or +2 kV/mm, respectively. Five bipolar or 10 unipolar measurement-cycles were applied before and after cycling. For one sample, 200 bipolar measurement-cycles were applied in order to observe the evolution of the polarisation and strain hysteresis under bipolar field after cycling. For the bipolar measurements the primary poling direction was the cycling direction and the unipolar measurements were conducted in cycling direction with the same polarity. Finally, for two samples with highest cycle number ($4.2{\cdot}10^8$ cycles) a unipolar measurement was conducted in the opposite direction of the cycling polarity after polarisation inversion (also at 40 mHz) in order to test the relaxation behaviour for reverse fields. The waiting time between the end of the cycling and the measurement was different from the previous measurements (about 2 weeks).

SEM images were taken from two samples with $4.2{\cdot}10^8$ cycles. Each of the samples was ground to different thicknesses using SiC powder. The surfaces were

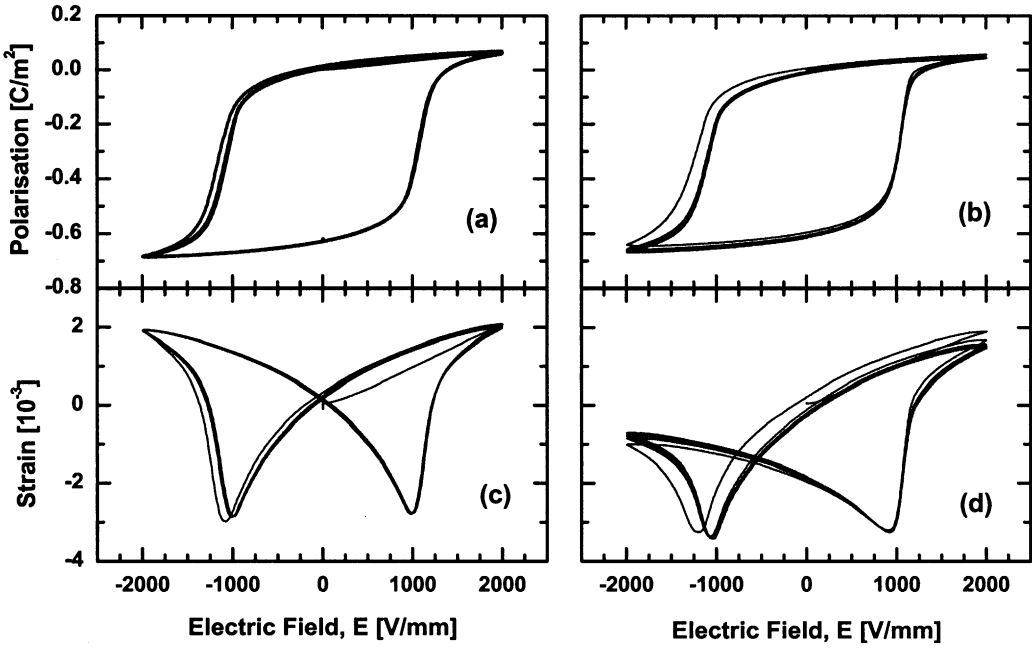

Fig. 1. Bipolar polarisation hysteresis (a) before and (b) after unipolar cycling ($3.2{\cdot}10^8$ cycles). The first five cycles are shown. (c) and (d) are the corresponding strain hysteresis loops.

then polished to 1 μm finish with diamond paste. The etching procedure was conducted such that the polished surfaces were wetted with HF/HCl. After about 60 s the surface was intensively rinsed with distilled water. A thin layer of Au/Pd was sputtered onto the samples to avoid charging in the SEM.

3. Results

3.1. Bipolar measurements

A direct comparison of the polarisation and strain hystereses is given in Fig. 1. The polarisation hysteresis exhibits a very slight decrease in remnant polarisation. The first hysteresis loop is shifted to the left and the next ones follow with a small continuous shift of the entire hysteresis to lower polarisation values. For each sample the strain hysteresis after cycling exhibits an asymmetry always in the same direction. The strain observed in cycling direction corresponding to the right wing (S_r) of the hysteresis loop is always higher than in the opposite direction (left wing, S_l).

As for the polarisation hysteresis the first loop deviates from the following ones. In the subsequent hysteresis loops a continuous decrease of S_r and an increase of S_l is observed. Thus consecutive bipolar cycles yield a gradual reduction of the strain asymmetry of a cycled sample.

In Figs. 2 and 3 the parameters obtained from the bipolar hysteresis loops are shown between 0 and

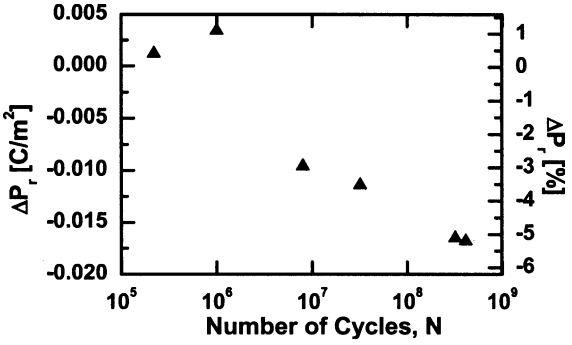

Fig. 2. Reduction of switchable polarisation due to unipolar cycling. The change of the total height of the hysteresis is plotted versus cycle number.

$4.2{\cdot}10^8$ cycles. The parameters of the third polarisation and strain hysteresis were evaluated because the first loop is not complete and differs from the following ones. The results were then averaged for three samples. According to Fig. 2 the remnant polarisation decreases steadily with cycle number. However, the decrease in P_r is small only reaching 5.2% of P_r after $4.2{\cdot}10^8$ cycles in comparison to the degradation induced by bipolar fatigue of around 70%.[3]

In Fig. 3 the strain values S_r, S_l and their ratio are shown. It is obvious that the asymmetry of the strain hysteresis increases with cycle number. Although the increase of the right wing is not so evident as the decrease of the left wing, the ratio, taken as a measure of the asymmetry, increases steadily with unipolar cycle number.

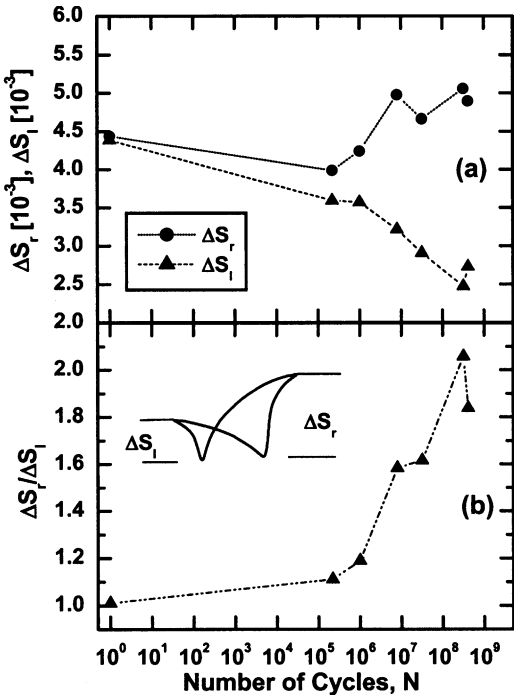

Fig. 3. (a) Strain amplitudes of the right (S_r) and left (S_l) wings of the strain hysteresis loops; (b) ratio of the right to left strain amplitudes.

Both intersections of the polarisation hysteresis with the field axis (coercive fields) slightly shift to more negative values with cycle number indicating a small shift of the entire hysteresis in the negative field direction. The shift observed in the polarisation hysteresis is somewhat smaller than the shift in the strain hysteresis, here determined from the minimum of the butterfly-loops (−19.4 V/mm after $3.2{\cdot}10^8$ cycles versus −69.8 V/mm for the strain hysteresis), both being only small fractions of the absolute coercive field values (1 kV/mm). As these values are determined during the third measurement hysteresis loop they represent a small remainder of an offset field.

3.2. Unipolar measurements

In Fig. 4 the unipolar polarisation and strain hysteresis are shown before cycling (a), (b) and after cycling, in cycling direction (c), (d), and in the opposite direction (e), (f). The polarisation hysteresis loops show a very slight decrease in slope in both directions after cycling. The slope of the strain hysteresis in cycling direction has increased whereas it has decreased in the opposite direction. It is more relevant to notice the differences between consecutive hysteresis measurements. For polarisation and strain of the uncycled sample, consecutive hysteresis loops steadily shift to higher strain or polarisation values, respectively. These shifts almost disappear after cycling indicating a completely saturated state of the sample without relaxation. Upon polarity inversion a second set of unipolar measuring cycles was applied to the samples. The relative shift of these hysteresis cycles at inverted polarity was significantly larger than before.

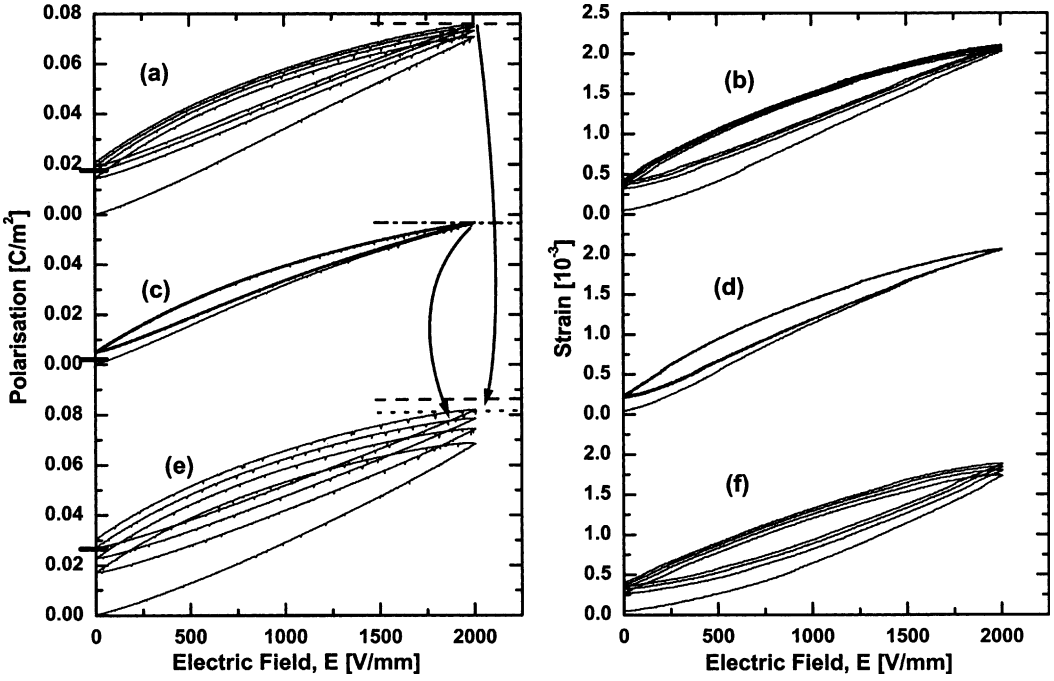

Fig. 4. Minor polarisation (left) and strain (right) hysteresis loops measured (a), (b) before unipolar cycling, (c), (d) after $4.2{\cdot}10^8$ unipolar fatigue cycles, and (d), (e) at opposite polarity after a single step of polarisation inversion. In order to illustrate the relative change of the strain amplitude, identical bottom markers are introduced on the left hand side of the plots. The markers on the right hand side indicate the differences in slope.

3.3. Multiple bipolar measurement cycles

200 bipolar hysteresis loops after unipolar cycling are shown in Fig. 5. The arrows indicate the shift in between consecutive loops. A shift of the polarisation hysteresis to lower polarisation values is observed for both the positive and negative polarity expressing a shift of the hysteresis loop as a whole. The strain measurements exhibit a steady removal of the asymmetry with a decrease of the right wing and an increase of the left wing. After 200 bipolar cycles the asymmetry is not yet completely removed. As shown in Fig. 6 the shifts of both hysteresis loops display an exponential dependence on the number of measurement cycles.

3.4. Microstructural changes

No significant changes were observed in the microstructure due to the unipolar fatigue. While bipolar fatigue is by now known to significantly modify the local affinity to etching of some grains allowing for an enhanced acid attack and showing etch grooves afterwards,[3,23] no differences between acid attacked virgin and unipolar fatigued samples were found.

4. Discussion

Our results show a much lower fatigue in unipolar cycled samples compared to bipolar cycled samples and agree with the measurements by Pan et al.[20] The degradation of the polarisation (ca. 5% after 10^9 cycles) is found to be much smaller than that observed after bipolar fatigue where the polarisation-decrease reaches 70% after 10^8 cycles. In a bipolar fatigued sample the total strain also strongly decreases with cycling, whereas it remains almost the same in a unipolar cycled sample, at least in one direction. The increase and the spreading of the coercive field characteristic of bipolar fatigue is not observed in the unipolar case where the strain minima remain sharp and the slope of the polarisation hysteresis at the coercive field is very steep.

The strong polarisation decrease in the bipolar fatigue can be explained by the pinning of domains through agglomerated point defects.[3,7,10] The large distribution of the clamping energies of the domains induces a large distribution of the coercive fields and as a consequence diffuse minima in the strain hysteresis. Unipolar cycling on the other hand seems to yield no strong pinning of the domains like in the bipolar fatigue and probably no

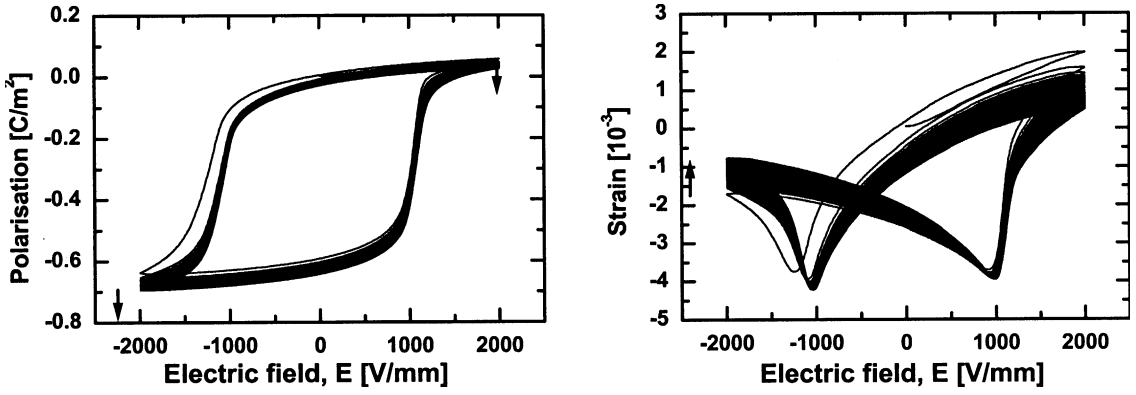

Fig. 5. Bipolar measurement cycles after 3.2×10^8 unipolar fatigue cycles: (a) polarisation, and (b) strain. 200 measuring cycles are shown.

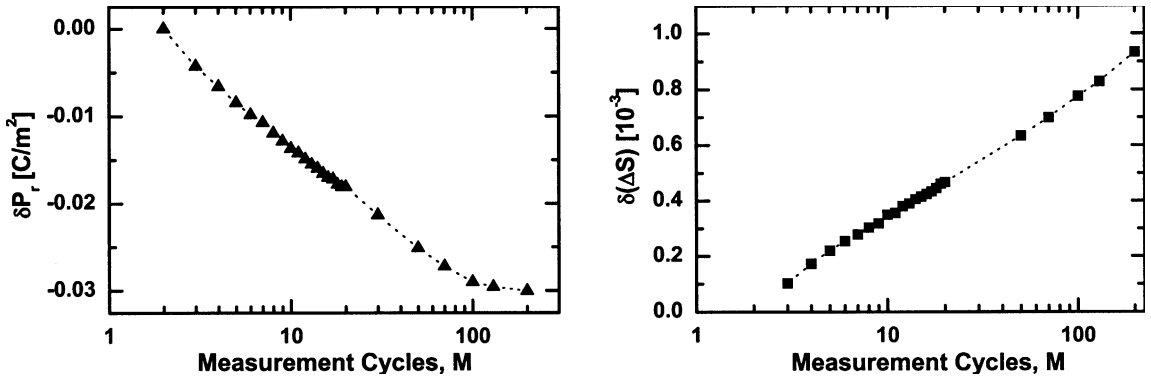

Fig. 6. (a) Reduction of the centre of the polarisation hysteresis loop measured as the average of the $+P_r$ and $-P_r$ corresponding to Fig. 5; (b) reduction of the maximum strain at 2 kV/mm as a function of measurement cycle number. Shown are the increase of the left wing, the reduction of the right wing and their average change.

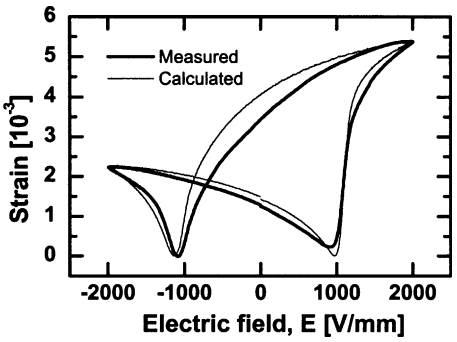

Fig. 7. Strain hysteresis loop after 3.2×10^8 cycles. Measured strain, and calculated strain by squaring the measured polarisation plus offset polarisation and re-scaling.

agglomeration of oxygen vacancies. The SEM images at least do not indicate any such formation.

The only common feature of the unipolar cycling with the bipolar one is the asymmetry of the strain hysteresis. This can be explained in both cases by the formation of an offset polarisation π in the bulk. Its existence is confirmed by the shift of the polarisation hysteresis loop to lower polarisation values, when a bipolar electric field is applied after unipolar cycling leading to a removal of this offset polarisation (Fig. 5).

According to Landau–Devonshire theory, the strain of an electrostrictive material is proportional to the square of the total polarisation (switchable and offset),[24] $S(E)=Q_{11}(P(E)\pm\pi)^2$. We obtain the approximated asymmetric butterfly curve as depicted in Fig. 7 for the parameters $Q_{11}=2.9.10^2$ m^4/C^2 and $\pi=0.074$ C/m^2. The degree of asymmetry depends on the value determined for π. Note, however, that the behaviour of the material is not purely electrostrictive, because the electrostricive hysteresis S–P curve is not perfectly parabolic. This calculation thus is only an approximation of the offset polarisation.

In the literature, a strain asymmetry was observed for a two layer model geometry modeling a multilayer geometry of cofired stack actuators[25] and attributed to the formation of cracks on one side of the sample. A vertical offset of the polarisation hysteresis was reported in aging and fatigue experiments. Warren et al.[8] explained the offset polarisation observed after aging by the local alignment of defect dipoles in the sense of the model description by Robels and Arlt.[6] The authors mention the implications of an offset polarisation on strain but no published data are cited. Kholkin et al.[18] gave a direct measure of an offset polarisation for PZT-thin films after bipolar fatigue. It was considered to be a buildup of fixed internal polarisation due to the pinning of ferroelectic domains in a preferred orientation. This was later correlated with observations showing fully clamped polarisation using atomic force microscopy.[13] The authors discuss that the mere alignment of defect dipoles is not a sufficient mechanism to account for the offset polarisation, because 10^{21} cm^{-3} dipoles would be needed to generate the effect. They furthermore observed that the offset polarisation is induced under bipolar fatigue, while unipolar fatigue induces an offset-field.

In our experiment, unipolar cycling yields both offsets but the effect of the offset polarisation is more pronounced than the offset field.

A characteristic difference between offset fields and offset polarisation is the degree of clamping of domains. If a domain is entirely clamped, its contribution will only be to enhance the total amount of aligned polarisation. A domain which is only partially clamped will actually react to the externally applied field, but at a modified field value. In the bulk material the offset field appears to be a weak microscopic mechanism, because it can be removed in a single bipolar cycle. All other offset fields then average out over the sample and effectively a non-shifted hysteresis loop is seen. This is different for the offset polarisation, which is obviously much more stable. Only the multitude of bipolar cycles in Fig. 5 unpins those domains, which during the unipolar fatigue developed into totally clamped domains constituting the offset polarisation. The 200 bipolar cycles shift the polarisation hysteresis loop by about 0.02 C/m^2. This is to be compared to the increase of the total height of 0.015 C/m^2, which is nearly the same amount. This implies that the lost offset polarisation has been re-gained for the polarisation switching. This argument supports the hypothesis of pinning of ferroelectric domains in a preferred direction, here the cycling direction. The pinning can result from the trapping of ionic and/or electronic defects[7,26] at domain walls locally stabilising these domains in a particular direction.[27] A second probable localisation for point charges within the microstructure is the grain boundary, where the charge mobility is comparatively high with respect to the bulk material. Values for strontium titanate yield values 30 times larger in the grain boundary than in the bulk,[1] but no study concerning this effect seems to be known for PZT. Due to the structural similarities of the perovskite ferroelectrics we expect similar ratios in PZT. Due to the assumed high charge mobility in the grain boundary, charges located here may be associated with the easily removable offset field while charges located within the grains fully stabilise the offset polarization. These may be freely located in some parts of the grain constituting a form of an electret effect.[28] The role of defect dipoles in our material is not evident due to the soft doping which has been considered to yield a material free of defect dipoles.

Altogether, the modifications of materials properties are significant enough to be unwanted in actuator applications. This becomes relevant particularly, when these actuators are incorporated into closed loop control systems, where the change in material properties then necessitates a sophisticated fatigue state dependent control circuitry.

5. Conclusion

Unipolar fatigue induces much lower losses of polarisation, but does induce a similar amount of offsets as bipolar fatigue. The underlying microscopic origins for the offset formation and for the loss in switchable polarisation are thus very likely to be different. The offsets induced during unipolar fatigue can be recovered by bipolar fields of the same amplitude, which is different in bipolar fatigued samples.

Acknowledgements

The authors thank Jürgen Nuffer for fruitful discussions. The support by the Deutsche Forschungsgemeinschaft through the "Schwerpunktprogramm Multifunktionswerkstoffe" (Lu729/4) is greatly acknowledged.

References

1. Scott, J. F., *Ferroelectric Memories*. Springer, Berlin, Heidelberg, 2000.
2. Uchino, K., *Piezoelectric Actuators and Ultrasonic Motors*. Kluwer Academic, Boston, Dordrecht, London, 1997.
3. Nuffer, J., Lupascu, D. C. and Rödel, J., Damage evolution in ferroelectric PZT induced by bipolar electric cycling. *Acta Mater*., 2000, **48**, 3783–3794.
4. Tagantsev, A. K., Stolichnov, I., Colla, E. L. and Setter, N., Polarization fatigue in ferroelectric films: basic experimental findings, phenomenological scenarios, and microscopic features. *J. Appl. Phys*., 2001, **90**(3), 1387–1402.
5. Robels, U. and Arlt, G., Domain wall clamping in ferroelectrics by orientation of defects. *J. Appl. Phys*., 1993, **73**, 3454–3460.
6. Robels, U., Schneider-Störmann, L. and Arlt, G., Dielectric aging and its temperature dependence in ferroelectric ceramics. *Ferroelectrics*, 1995, **168**, 301–311.
7. Brennan, C., Model of ferroelectric fatigue due to defect/domain interactions. *Ferroelectrics*, 1993, **150**, 199–208.
8. Warren, W. L., Dimos, D. and Waser, R. M., Degradation mechanism in ferroelectric and high-permittivity perovskites. *MRS Bulletin*, 1996, **21**(7), 40–45.
9. Warren, W. L., Dimos, D., Tuttle, B. A. and Smyth, D. M., Electronic and ionic trapping at domain walls in $BaTiO_3$. *J. Am. Ceram. Soc*., 1994, **77**(10), 2753–2757.
10. Scott, J. F. and Dawber, M., Oxygen-vacancy ordering as a fatigue mechanism in perovskite ferroelectrics. *Appl. Phys. Lett*., 2000, **76**, 3801–3803.
11. Scott, J. F. and Dawber, M., New interface effects in ferroelectric thin films. *J. Phys. IV France*, 2001, **11**, Pr11-9–Pr11-19.
12. Levstik, A., Kosec, M., Bobnar, V., Filipic, C. and Holc, J., Switching kinetics in thick film and bulk lead lanthanum zirconate titanate ceramics. *Jpn. J. Appl. Phys*., 1997, **36**, 2744–2746.
13. Colla, E. L., Hong, S., Taylor, D. V., Tagantsev, A. K. and Setter, N., Direct observation of region by region suppression of the switchable polarization (fatigue) in Pb(Zr, Ti)O_3 thin film capacitors with Pt electrodes. *Appl. Phys. Lett*., 1998, **72**(21), 2763–2765.
14. Ganpule, C. S., Roytburd, A. L., Nagarajan, V., Hill, B. K., Ogale, S. B., Williams, E. D., Ramesh, R. and Scott, J. F., Polarization relaxation kinetics and 180° domain wall dynamics in ferroelectric thin films. *Phys. Rev. B*, 2001, **65**, 014101-1-7.
15. Winzer, S. R., Shankar, N. and Ritter, A. P., Designing cofired multilayer electrostrictive actuators for reliability. *J. Am. Ceram. Soc*., 1989, **72**, 2246–2257.
16. Furuta, A. and Uchino, K., Destruction mechanism of multilayer ceramic actuators: case of antiferroelectrics. *Ferroelectrics*, 1994, **160**, 277–285.
17. Khamankar, R. B., Kim, J., Sudhama, C., Jiang, B. and Lee, J. C., Effects of electrical stress parameters on polarization loss in ferroelectric P(L)ZT thin film capacitors. *IEEE Electron Dev. Lett*., 1995, **16**(4), 130–132.
18. Kholkin, A. L., Colla, E. L., Tagantsev, A. K., Taylor, D. V. and Setter, N., Fatigue of piezoelectric properties in Pb(Zr,Ti)O_3 films. *Appl. Phys. Lett*., 1996, **68**(18), 2577–2579.
19. Lee, S. C., Teowee, G., Schrimpf, R. D., Birnie III, D. P., Uhlmann, D. R. and Galloway, K. F., Fatigue effect on the I-V characteristics of sol-gel derived PZT thin films. In *ISAF'92, Proc. Eighth IEEE Int. Symp. Appl. Ferroel*., ed. M. Liu, A. Safari, A. Kingon and G. Heartling. IEEE, New York, USA, 1992, pp. 240–245.
20. Pan, W., Yue, C.-F. and Tosyali, O., Fatigue of ferroelectric polarization and the electric field induced strain in lead lanthanum zirconate titanate ceramics. *J. Am. Ceram. Soc*., 1992, **75**(6), 1534–1540.
21. Chikarmane, V., Sudhama, C., Kim, J., Lee, J., Tasch, A. and Novak, S., Effects of post-deposition annealing ambient on the electrical characteristics and phase transformation kinetics of sputtered lead zirconate titanate (65/35) thin film capacitors. *J. Vac. Sci. Technol*., 1992, **10**(4), 1562–1568.
22. Carrano, J., Sudhama, C, .Lee, J., Tasch, A. and Miller, W., Electrical and reliability characteristics of lead-zirconate-titanate (PZT) ferroelectric thin films for DRAM applications. *Int. Electr. Device Meeting, Techn. Digest., 1989, 255–258*.
23. Nuffer, J., Lupascu, D. C., Glazounov, A., Kleebe, J.-J. and Rödel, J., Microstructural Modifications of ferroelectric lead zirconate titanate ceramics due to bipolar electric fatigue. *J. Eur. Ceram. Soc*., 2002, **22**(13), 2133–2142.
24. Grindlay, J., *An Introduction to the Phenomenological Theory of Ferroelectricity*. Pergamon Press, Oxford, 1970.
25. Furuta, A. and Uchino, K., Dynamic observation of crack propagation in piezoelectric multilayer actuators. *J. Am. Ceram. Soc*., 1993, **76**, 1615–1617.
26. Warren, W. L., Dimos, D., Tuttle, B. A., Pike, G. E., Schwartz, R. W., Clews, P. J. and McIntyre, D. C., Polarization suppression in Pb(Zr, Ti)O_3 thin films. *J. Appl. Phys*., 1995, **77**, 6695–6701.
27. Shur, V., Rumyantsev, E., Nikolaeva, E., Shishkin, E., Baturin, I., Lupascu, D. C., Randall, C.A. and Ozgul, M. Fatigue effect in bulk ferroelectrics. In *Smart Structures and Materials: Active Materials: Behavior and Mechanics*, ed. C. S. Lynch. *Proc. SPIE* 2002, **4699**, 40–50.
28. Sessler, G.M., Ed., *Electrets*. Springer, Heidelberg, New York, 1987.